Soft Matter

Accepted Manuscript

ROYAL SOCIETY OF CHEMISTRY

www.rsc.org/softmatter

The microstructure and rheological properties of microfibril networks can be controlled by using an adsorbing charged polymer in combination with mechanical de-agglomeration.

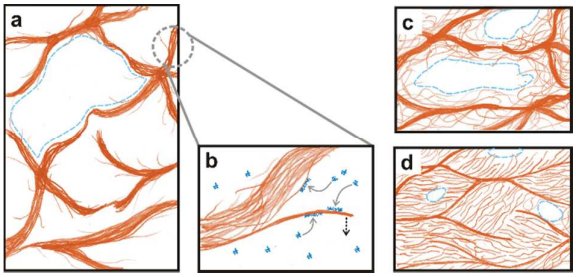

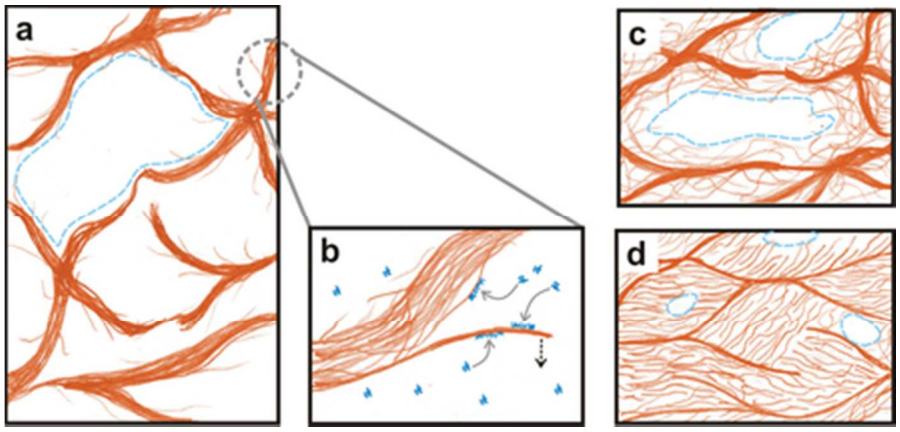

37x17mm (300 x 300 DPI)

Cite this: DOI: 10.1039/c0xx00000x

www.rsc.org/xxxxxx

ARTICLE TYPE

Microstructure and rheology of microfibril-polymer networks

Sandra J. Veen*[a], Peter Versluis[a], Anke Kuijk[a] and Krassimir P. Velikov*[a,b]

Received (in XXX, XXX) Xth XXXXXXXXX 20XX, Accepted Xth XXXXXXXXX 20XX
DOI: 10.1039/b000000x

By using an adsorbing polymer in combination with mechanical de-agglomeration, the microstructure and rheological properties of networks of microfibrils could be controlled. By the addition of sodium carboxymethyl cellulose during de-agglomeration of networks of bacterial cellulose, the microstructure could be changed from an inhomogeneous network with bundles of microfibrils and voids to a more homogeneous spread and alignment of the particles. As a result the macroscopic rheological properties were altered. Although still elastic and gel-like in nature, the elasticity and viscous behavior of the network as a function of microfibril concentration is altered. The microstructure is thus changed by changing the surface properties of the building blocks leading to a direct influence on the materials macroscopic behavior.

The intricate connection between the microstructure and the macroscopic properties of a material is both of interest from a fundamental point of view (for instance in the understanding of biological systems) as well as for industrial applications. In fact, controlling the microstructure is essential in the design of new materials. One way of changing the microstructure, and with it a material's properties, is the use of long anisotropic particles as a scaffold in particle/polymer composites. Examples include carbon nanotubes, actin filaments and even cellulose microfibrils for enforced composites with improved mechanical or conducting properties.[1,2,3] Cellulose microfibrils (CMF) in particular are an increasingly important natural material used in many industrial applications.[4] This is in part because it originates from renewable sources such as plants or from some bacteria. Bacterial cellulose (BC) in specific is a very attractive model system due to its purity. Bacteria of the strain Aceto Bacter form large ribbon-shaped CMFs (~60 nm wide, ~9 nm thick and up to several micrometers long) by building up the polysaccharides from the glucose molecules they consume.[5] Native BC is present in pellicles in which the CMFs form networks due to strong attractions (~ 10kT/μm at a distance of 10 nm) between them[6]. These attractions originate from surface OH-group mediated hydrogen bonds and Van der Waals interactions.[7] Using mechanical de-agglomeration, the microfibrils can be separated but due to their attractive nature they readily aggregate or re-form system spanning networks. These networks have been shown to be elastic in nature and to consist of large bundles of microfibrils[6].

Fibrillar particles like CMFs can be used to alter the properties of a polymer network by mixing in their own network properties. Here a reversed approach is employed in which an adsorbing polymer is added during mechanical de-agglomeration in order to change the properties of the CMFs and the resulting network. Carboxymethyl cellulose (CMC) is a charged polymer with a known affinity for the cellulose surface.[8,9] It has been shown to be a good dispersant for CMFs when added during mechanical de-agglomeration of the network.[10] In this paper, we investigate the change in microstructure of CMF networks due to the adsorption of CMC onto BC and the resulting effect on the macroscopic rheological properties.

Cubes of BC in syrup from eight cups with 220 mL of lychee/vanilla flavored nata de coco (Kara Santan Pertama, Bogor 16964, Indonesia) were filtered and washed under a demi-water tap. After immersion in 1.5 L of nanopure water (Barnstead Nanopure Diamond, resistance 18 MΩ-cm) the cubes were cut by a hand blender (Braun 4185545) and washed. Each washing step consisted of rinsing the cellulose by filtration over a vacuum filter (Whatman Schleicher and Schuell 113, wet strengthened circles, 185 mm diameter) and redispersing the residue in 1.5 L of nanopure water with the hand blender. After eight washing steps the cellulose residue was redispersed in 400 mL of nanopure water. Several samples containing a volume fraction (ϕ) of ~5×10^{-3} of BC (weight percent (wt%) 0.8, density of BC=1.5 g/mL[11]) were prepared by dilution with nanopure water and adding different amounts of a concentrated CMC solution (Ashland Blanose Aqualon 99.5% pure, 9M31XF, M_w ≈250 000 g/mol, degree of polymerization = 1100, degree of substitution = 0.8-0.95, density 0.75 g/mL). These samples were passed through a Microfluidizer once (M110S, Microfluidics) with a z-chamber of 87 μm at a pressure of 1200 bar. The wt% of BC in the resulting mixtures was determined gravimetrically by drying of the dispersions under reduced pressure and elevated temperatures. The average over three samples per CMC/BC ratio was taken. Concentration series were made by dilution with nanopure water and redispersion by gentle agitation (shaking).

Rheological measurements of the CMC/BC suspensions were performed on a stress controlled rheometer (AR G2 or AR 2000, TA Instruments), using a plate-plate geometry (plate diameter 4 cm, gap 1 mm). Sand-blasted metal plates were used to prevent wall slip. The system was temperature controlled with a peltier system at a temperature of 20 ± 0.1°C. A time sweep was performed by imposing an oscillatory shear with a frequency of 1 Hz and 0.1% strain. Flow measurements were performed in which the shear rate was first increased from 0.1 to 500 s^{-1} in 2 min and then decreased from 500 to 0.1 s^{-1} in 2 min.

Measurements were repeated four times for the complete pure BC series and three times for the different CMC/BC ratios at ϕ~2.7×10^{-3}. Frequency sweeps were performed in the range of 0.01−100 rad/s at a strain of 0.1% (see Supplementary Information (SI)). The continuous phase of the CMC/BC suspensions was obtained by centrifugation in Eppendorf safe-lock tubes of 2.0 mL in a Heraeus Biofuge Primo R for 4:45 hours at a speed of 13000 rpm and a temperature of 20°C. Viscosity measurements of the supernatants were performed on an Anton Paar Physica MCR301 rheometer, using a plate-plate geometry (plate diameter 25 mm, gap 0.1 mm). The zero shear viscosity at 20°C was determined by increasing the shear rate from 100 to 1×10^5 s^{-1} and fitting the obtained curve to a Cross/Williamson model (see SI). Confocal scanning laser microscopy (CSLM) was performed on a Leica TCS-SP5 confocal microscope. For staining, ~10 µL of 0.5 w/v% congo red solution in water was added to 1 mL of dispersion. For imaging, the samples were placed between two cover slips separated by a (3 mm) spacer. Image analysis was performed in ImageJ[12] (details see SI). Images between crossed polarizers and under bright light illumination were taken in 0.5 cm thick optical glass cuvettes.

In previous research is has been shown that adding CMC during mechanical de-agglomeration of BC networks leads to adsorption of the charged polymer and a subsequent change of the surface properties of the obtained microfibrils.[10] At low concentrations of BC this led to dispersions of individual microfibrils. To investigate the effect of this process on the microstructure of networks of BC, suspensions at different CMC/BC weight ratios were prepared. The ratios ranged from 0 (i.e. pure BC) to 0.250 (~1.47 mg CMC per m^2 surface area of BC, see SI). The microstructure was imaged with confocal microscopy at two different BC volume fractions, namely ϕ~1×10^{-3} and ~5×10^{-3}. The results for ϕ~5×10^{-3} are given in fig. 1 (see SI for ϕ~1×10^{-3}).

As the CMC content increases, the network contains less and smaller voids (white areas in fig. 1a-e) as well as less bundles of microfibrils (black rod like areas in fig. 1a-e). The addition of CMC during de-agglomeration clearly results in a more homogeneous network. This effect can be quantified by taking the full width at half maximum (FWHM) of the normalized intensity distribution of the confocal images (see SI). A higher value indicates a more homogeneous system. The results are given in fig. 2a. The analysis was done on images at 40 times magnification of suspensions containing both a ϕ~1×10^{-3} and ~5×10^{-3} BC. As can be seen, the FWHM increases from 0.03 to 0.3 for ϕ~5×10^{-3} and from 0.01 to 0.2 for ϕ~1×10^{-3}. The addition of CMC thus leads to an improved spread of the microfibrils.

The CMC not only improves the spread of the microfibrils, it also promotes their alignment. This can be seen by placing the suspensions between crossed polarizers (fig. 1f). Under regular bright light the samples look homogeneously white. When viewed between crossed polarizers however, clear white and dark regions are seen indicating alignment of the microfibrils. This is, for instance, seen when elongated particles align with their long axis in the same direction which is known as nematic-type ordering[13]. Initially the only alignment of the fibrils is in the large bundles. Upon increase of the CMC content domains of aligned fibrils grow and colors become visible indicating an increase in alignment and/or domain size.[14] The amount of nematic alignment can be quantified by measuring the distribution of orientation angles of the microfibrils in the confocal images (see SI).[15] From this the two dimensional order parameter $S_{2D} = \sqrt{\langle \sin 2\theta \rangle^2 + \langle \cos 2\theta \rangle^2}$ was calculated (brackets indicate average values, θ is angle between fibril and image horizontal plane).[16] A value of 0 means a completely random orientation, while a value of 1 indicates complete alignment. Fig. 2b shows that increasing the CMC content indeed increases the alignment of the microfibrils.

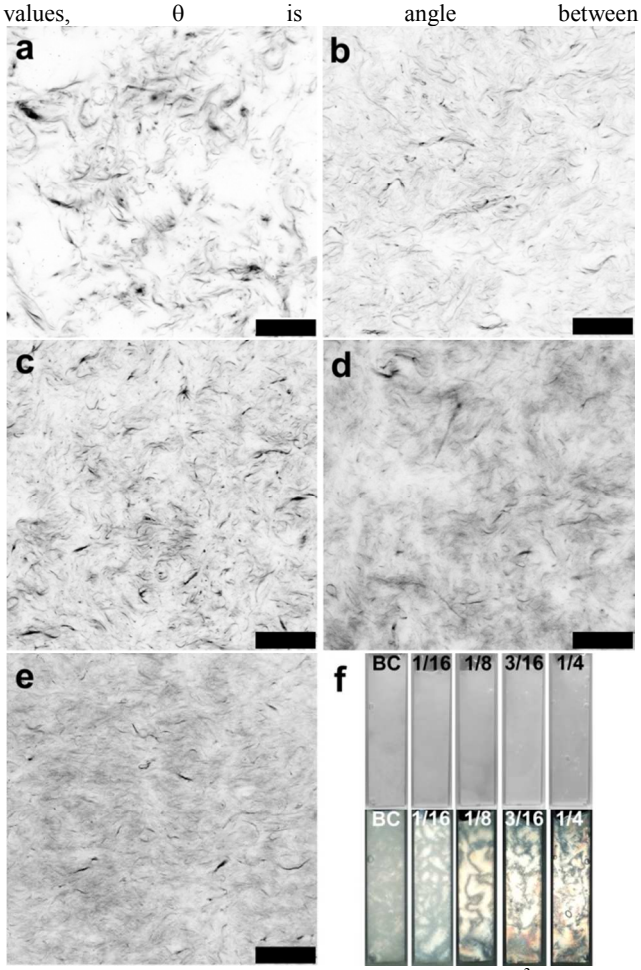

Fig. 1 Confocal images of microfibril networks at ϕ~5×10^{-3} BC. From a to e the CMC/BC ratio increases from 0, 1/16, 1/8, 3/16 to ¼. Scale bar = 75 µm. Images are inverted for clarity. f) Images of networks of microfibrils at ϕ~5×10^{-3} BC under bright light illumination (top) and between crossed polarizers (bottom) at different CMC/BC ratios.

Adding CMC during de-agglomeration of the BC network has a profound effect on the formed microstructure. To investigate the effect on the macroscopic properties, rheological measurements were performed. At least 8 different BC concentrations were used ranging from ϕ~0.7×10^{-3} to ~5×10^{-3} at different CMC/BC ratios. Typical flow curves under shear of these suspensions are shown in fig. 3a/b. Here the relative viscosity $\eta_{rel} = \eta/\eta_s$ (η = viscosity of the suspension, η_s= viscosity of the continuous phase containing non-adsorbed CMC) is given as a function of the shear rate. The viscosity of the supernatant was constant in the shear rate range measured for the CMC/BC suspensions (see SI). The flow curves show a strong shear thinning behavior. This is characteristic for all suspensions, regardless of their CMC/BC ratio and BC concentration. None of

the suspensions showed a Newtonian plateau at low shear rates over the measured concentration range. Fig. 3c-f show the frequency dependence of the elastic modulus (*G'*) and loss modulus (*G"*) for pure BC as well as CMC/BC 0.185.[6] *G'* is larger than *G"* for all concentrations for both suspensions. The suspensions are thus predominantly elastic.

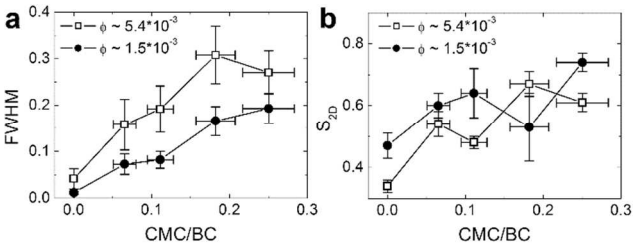

Fig. 2 (a) Full width at half maximum (FWHM) of the normalized intensity distribution of the confocal images. (b) Two dimensional order parameter S_{2D} calculated using the same confocal images. Error bars are one standard deviation.

Furthermore, *G*' reaches a nearly frequency independent plateau value for both CMC/BC ratios. For pure BC, *G*" starts with a plateau followed by an increase with measurement frequency ($G" \sim \omega^{0.2-0.5}$) while for a ratio of 0.185 only a slight increase is seen. This behavior indicates that the measurements are in the intermediate frequency regime and shows the characteristics of a strong gel with the BC concentration controlling the gel strength.[17] This behavior has also been observed for other fibril networks such as actin and carbon nanotubes.[18]

Although a surprising result at first, at high BC concentrations and high CMC content it has been shown that a nematic gel-type structure is formed.[10] Despite an increase in particle alignment, this structure still acts as a gel: an arrested state and non-equilibrium structure. Measuring the viscoelastic properties of gels is notoriously difficult, since the results depend on both the preparation as well as the shear history of the sample. Due to the non-equilibrium nature of the network structure, the properties of a gel can slowly change over time. This is for instance seen in a slow but gradual change of both *G*' and *G*". An example of this time dependence is given in Figure 3. The change in *G'* (Fig.3g) and *G*" (Fig.3h) is shown for four different CMC/BC ratios at similar ϕ of BC. The G' continuously increases while *G*" decreases in time. This change persists for at least 18 hours and does not saturate within this timeframe. Longer measurements were not possible due to drying of the sample. It is believed that this gradual change is due to a slow reformation of contacts between the microfibrils after they are disturbed by the lowering of the top plate before a rheological measurement (see SI). It is therefore important to treat time as an additional parameter and make a comparison of the viscoelastic properties within the same timeframe. By taking *G*' and *G*" as measured after, for instance, 5 minutes reproducible results could be obtained for all suspensions.

Gels are often characterized by the concentration dependence of *G*'. Several theories based on either colloidal percolation or polymer theory predict a power-law dependence with exponents of ~2 or slightly higher.[19,20] Experimentally, the exponents can vary quite extensively. For instance, values between 2 and 7 can be found for carbon nanotube networks depending on their treatment and solvent conditions.[1] CMFs obtained from wood cellulose have been shown to have an exponent of ~3.[21] For the BC systems, the concentration dependence of *G*' and $G"\text{-}\eta_s\omega$ are given in fig. 4. For *G"*, it has to be kept in mind that not all the CMC added to the system adsorbs onto the microfibril surface during mechanical treatment.[10] Part of the polymer still remains in the continuous phase of the suspension and thereby increases its viscosity η_s. To retrieve the viscous contribution of the CMC/BC particles, the contribution of the continuous phase can simply be subtracted from the total by taking $G"\text{-}\eta_s\omega$.[17] The concentration dependencies of G' and $G"\text{-}\eta_s\omega$ were fitted to a power-law of the form ϕ^n. The obtained exponents *n* for all CMC/BC ratios are shown in fig. 4c. For the elastic modulus, *n* ranged from 3.53 ± 0.06 for pure BC to, on average, 3.17 ± 0.10 for the systems with added polymer. The values for *n* and the fit for pure BC and ratio 0.185 are also given in fig. 4a. For $G"\text{-}\eta_s\omega$ the exponent gradually decreases from 3.31 ± 0.08 without CMC to 2.80 ± 0.11 for CMC/BC 0.185 (fig. 4b/c).

The aforementioned theories for the concentration dependence of *G'* only take into account the contribution of stretching and compression of particles under shear as the source of the network elasticity. Cross-linked networks of semi-flexible polymers, however, may also have contributions from bending.[22] Semi-flexible polymers have a persistence length which is shorter than their contour length but larger than their diameter. They are thus rigid on a small scale while still flexible on a long scale. This results in qualitatively different elastic and viscoelastic properties as compared to regular polymers. Taking bending energetics into account in 3D models is not straightforward and results for the concentration dependence of *G'* are often given in bending or stretching dominated regimes. For instance, 3D lattice models give exponents of 2.6 (semi-flexible) to 3 (stiff fibres) for bending dominated elasticity.[23] The exponent of 3 is close to what is found

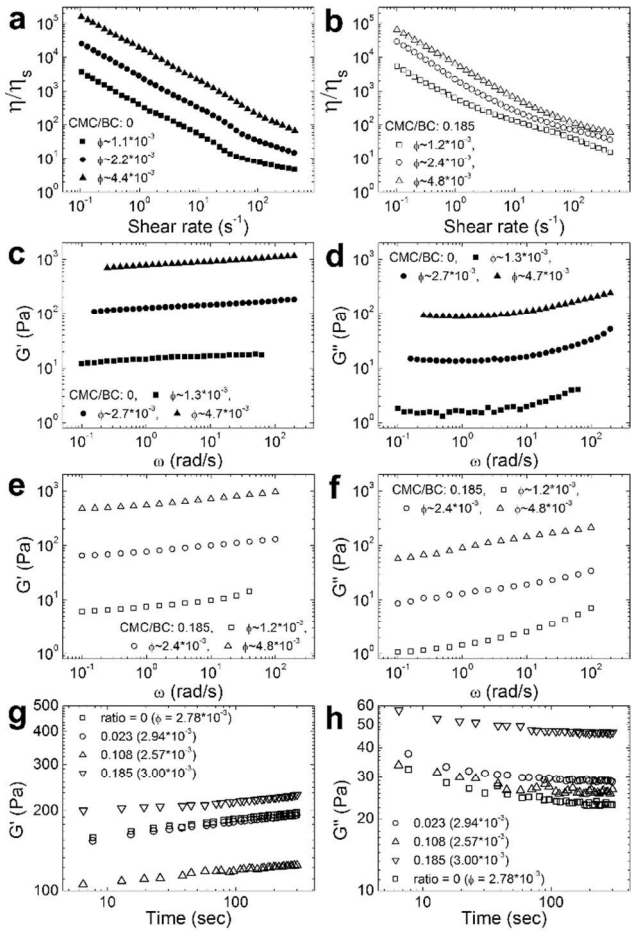

Fig.3 Viscoelastic properties of BC networks (a/b) Viscosity as a function of shear rate. (c/e) Elastic (*G'*) and loss (*G''*) modulus as a function of frequency. (g/h) G' and *G''* in time for four different CMC/BC ratios at similar volume fractions (ϕ) of BC.

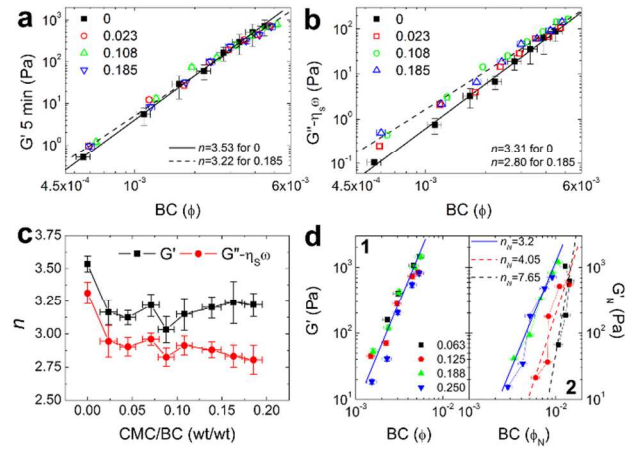

Fig.4 (a/b) *G'* and *G''*-$\eta_s\omega$ as a function of BC concentration. Different symbols indicate different CMC/BC ratios. Error bars: 95.45% accuracy. (c) Exponents *n* from the power-law fit of the moduli as a function of concentration (error bars: one standard deviation). (d) Power-laws for selected CMC/BC ratios before (d1) and after (d2) normalization with void concentration.

for the CMC/BC mixtures, suggesting that the elasticity of these networks may be bending dominated.

The exponent for pure BC, however, is much larger. In the aforementioned lattice models, the network has an ordered structure and it is assumed that cross-links/bonds are freely hinged and can thus rotate and change angle. The confocal images for pure BC do not show such an ordered structure. In fact, the network is highly inhomogeneous. A scaling theory which incorporates a random network rather than an ordered one, leads to an exponent of 11/3≈3.67 for low CMF concentrations.[19] This is closer to the obtained n=3.53. Simulations on elastic percolation models with bonds that resist stretching and rotation lead to the even higher *n* of 3.75.[24] The network structure in this case was described as consisting of quasi-1D strings connected to one another by nodes (blobs of multiple bonds). This suggests that for the pure BC, not only microfibril bending but also the network inhomogeneity and the strong attractions between the microfibrils play a crucial role in the network elasticity.

The presence of voids can influence the power-law concentration dependence of *G'*. It is known that voids can change *G'* by orders of magnitude.[19,25] To determine the elasticity of the macroscopically homogeneous network (i.e. void free part), the volume fraction of voids ξ_V needs to be known. An estimate of ξ_V was made from 3D binary reconstructions of the network from confocal images (see SI). The system was considered to consist of two parts: a macroscopically homogeneous network part containing fibrils and a void part without fibrils. Knowing ξ_V, the volume fraction of BC in the network ($\phi_N = \phi/(1-\xi_V)$) as well as its elastic modulus (G'_N) could be determined (see SI). G'_N was calculated by making use of the Reuss-Voigt-Hill averaging scheme which is frequently used in material science to predict the elastic modulus of composite materials containing fiber-like constituents such as cellulose fibrils and whiskers.[19,25–30] This was done by using a weighted mean of the properties of the different parts of the composite, in this case the microfibril network part and the voids (see SI).

Fig. 4d shows the original and normalized power-laws for four different CMC/BC ratios. For the two lowest ratios, the power-law exponent changes significantly. From n ~ 3.17 before taking into account the presence of voids, to n_N=7.65 at CMC/BC 0.063 and n_N=4.05 at CMC/BC 0.125 after normalization. Such high exponents are, for instance, also seen for systems of carbon nanotubes.[1] For CMC/BC ratios of 0.188 and 0.125 the exponent remains ~3,17. Accounting for the presence of voids results in a decrease of n_N with an increase in alignment and homogeneity of the microstructure as a result of an increase in CMC

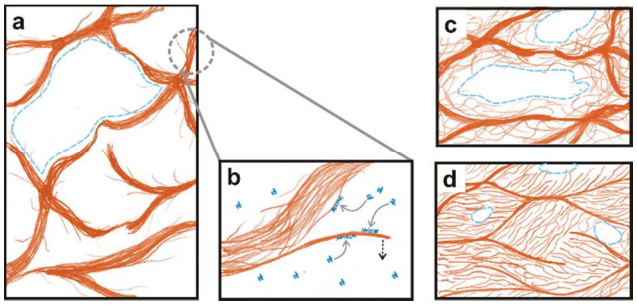

Fig.5 A) Original 3D network of bundles and aggregates of microfibrils. Blue dashed lines indicates void space. B) Individual microfibrils can be detached from larger bundles during de-agglomeration. CMC from solution (dark blue) can adsorb onto microfibrils surface. Microstructures after de-agglomeration: (C) low CMC/BC ratios (D) high CMC/BC ratios with nematic type ordering.

concentration. This is direct evidence for a change in the interactions between the fibrils in the macroscopically homogeneous regions when the adsorbing charged polymer is added. Using different averaging schemes for the calculation of G_N' or different approaches in the determination of ξ_V does not alter the observed trend in n_N with CMC/BC ratio (see SI). Interestingly, n_N remains unchanged after reaching the CMC/BC ratio at which at low concentrations a transition from aggregates in solution to nematic type ordering is seen.[10]

Another result evident from fig. 4d is that for the same ϕ_N of BC, G_N' increases with increasing CMC/BC ratio. A more elastic network is obtained with increasing number of free microfibrils. Comparable behavior has been observed for a system of rods in which the reverse transition is induced: from repulsive rods to a network of bundles of attractive rods.[31] The increase in *G'* is attributed to the increase in the number of particle contacts due to a change in the "particle" that builds up the network: bundles of attractive rods versus single repulsive rods. The major difference is that in the CMC/BC systems this effect is found for the macroscopically homogeneous part (i.e. after taking into account the void volume), but is hardly noticeable for the macroscopic sample as a whole (Fig. 4a).

The comparison to known theories shows that the interpretation of the rheological properties of microfibril-polymer networks is not straightforward. The observed change in time of the moduli poses additional complications. A glassy network of wormlike chains incorporates this behavior, but rheological descriptions remain phenomenological.[22] What is clear is that the microstructure of the microfibril networks changes with increasing CMC addition during de-agglomeration. As mentioned before, at low BC concentrations a transition from attractive to repulsive interactions for individual microfibrils is found.[10] At higher fibril concentrations, however, the presence of additional attractive forces (e.g. bridging interactions or a lowering of repulsive barrier due to increase in ion concentration) or physical entanglement of the semi-flexible particles cannot be ruled out.

It is important to point out that the presented systems are not produced by destabilizing a colloidal dispersion of elongated particles. In fact, the starting point is a highly aggregated and inhomogeneous state (i.e. 3D network of bundles and aggregates of microfibrils) (Fig.5a). This network is subjected to high energy mechanical treatment in an attempt to pull the fibrils in the bundles apart. In attractive systems the resulting microstructure can be strongly depended on shear history. The mechanical treatment, however, does not guarantee full de-agglomeration: aggregates and bundles from the original inhomogeneous network could still be present (as is evident from the confocal images). During mechanical treatment, individual microfibrils can be detached from larger bundles exposing new surfaces at which the CMC can adsorb (Fig.5b). We hypothesize that the systems obtained after de-agglomeration contain structures formed by CMC-altered microfibrils and voids, as well as the larger bundles remaining from the original structure (Fig. 5c/d). These larger bundles can contribute to the elastic response of the system. The different amounts of adsorbed CMC lead to differences in the observed microstructure in which increased repulsive contributions may still play a role. The overall macro-scale structure, however, remains highly heterogeneous owning to incomplete de-agglomeration resulting in the presence of bundles and voids.

The complexity of the obtained structures makes it difficult to compare observed structural changes to known transitions, for instance gel to glass transitions in dispersions of rod-like particles.[32] The microfibrils are also more flexible than rod-like in nature and are highly polydisperse in length (aspect ratio from 46 to 646).[10] Considering the volume fraction in the network part (from ~10^{-3} to ~10^{-2}) and the average aspect ratio of 250, previous research has shown that transitions from (attractive) gels to (repulsive) glasses are likely to occur for the CMC/BC systems. [32] It is, however, clear that further research is imperative to obtain a better understanding of the elasticity of mixed fibril-polymer networks.

In conclusion, it has been shown that by the addition of CMC during mechanical de-agglomeration of networks of BC microfibrils, the microstructure can be changed: from an inhomogeneous network with bundles of microfibrils and voids to a more homogeneous spread and alignment of the particles. Yet, the overall macro-scale structure remains heterogeneous due to incomplete de-agglomeration. As a result the macroscopic rheological properties were altered. Although still elastic and gel-like in nature, the elastic as well as the viscous behavior of the system as a function of BC concentration changes under influence of the CMC. The microstructure is thus changed by altering the surface properties of the building blocks leading to a direct influence on the materials macroscopic behavior. Taking into account the presence of voids, the power-law concentration dependence of *G'* of the fibril-polymer network changes significantly. This provides evidence for a change in the interactions between the micro-fibrils. Finally, the obtained insights may help in altering the material properties of composites containing fibrillar particles and offers an alternate route to new material design.

This research was financially supported by NanoNextNL. C. Storm and G. Koenderink are thanked for a critical review of the manuscript and helpful input.

[a] *Unilever R&D Vlaardingen, Olivier van Noortlaan 120, 3133 AT Vlaardingen, The Netherlands. E-mail: sandra.veen@unilever.com, krassimir.velikov@unilever.com*

[b] *Soft Condensed Matter, Debye Institute for Nanomaterials Sciene, Department of Physics and Astronomy, Utrecht University, Princetonplein 1, 3584 CC Utrecht, The Netherlands.*

1 E. K. Hobbie, *Rheol. Acta*, 2010, **49**, 323–334.
2 J. Xu, S. Chatterjee, K. W. Koelling, Y. Wang and S. E. Bechtel, *Rheol. Acta*, 2005, **44**, 537–562.
3 A. B. Fall, S. B. Lindström, J. Sprakel and L. Wågberg, *Soft Matter*, 2013, **9**, 1852–1863.
4 I. Siró and D. Plackett, *Cellulose*, 2010, **17**, 459–494.
5 U. Geyer, T. Heinze, A. Stein, D. Klemm, S. Marsch, D. Schumann and H. P. Schmauder, *Int. J. Biol. Macromol.*, 1994, **16**, 343–347.
6 A. Kuijk, R. Koppert, P. Versluis, G. van Dalen, C. Remijn, J. Hazekamp, J. Nijsse and K. P. Velikov, *Langmuir*, 2013, **29**, 14356–14360.
7 D. Klemm, B. Heublein, H.-P. Fink and A. Bohn, *Angew. Chem. Int. Ed. Engl.*, 2005, **44**, 3358–3393.
8 H. Yamamoto and F. Horii, *Cellulose*, 1994, **1**, 57–66.
9 C. H. Haigler, A. R. White, R. M. Brown and K. M. Cooper, *J. Cell Biol.*, 1982, **94**, 64–9.

10 S. J. Veen, A. Kuijk, P. Versluis, H. Husken and K. P. Velikov, *Langmuir*, 2014, **30**, 13362–13368.
11 C. Sun, *J. Pharm. Sci.*, 2005, **94**, 2132–2134.
12 C. A. Schneider, W. S. Rasband and K. W. Eliceiri, *Nat. Methods*, 2012, **9**, 671–675.
13 L. Onsager, *Ann. New York Acad. Sci.*, 1949, **51**, 627–659.
14 M. Born and E. Wolf, *Principles of Optics, Electromagnatic Theory of Propagation, Interference and Diffraction of Light*, Pergamon Press, Fourth Edi., 1970.
15 R. Rezakhaniha, A. Agianniotis, J. T. C. Schrauwen, A. Griffa, D. Sage, C. V. C. Bouten, F. N. van de Vosse, M. Unser and N. Stergiopulos, *Biomech. Model. Mechanobiol.*, 2012, **11**, 461–473.
16 J. Alvarado, B. M. Mulder and G. H. Koenderink, *Soft Matter*, 2014, **10**, 2354–2364.
17 R. G. Larson, *The structure and rheology of complex fluids*, Oxford University Press, New York, Oxford, 1999.
18 K. W. Müller, R. F. Bruinsma, O. Lieleg, A. R. Bausch, W. A. Wall and A. J. Levine, *Phys. Rev. Lett.*, 2014, **112**, 238102.
19 R. J. Hill, *Biomacromolecules*, 2008, **9**, 2963–2966.
20 M. Doi and S. F. Edwards, *The theory of polymer dynamics*, Oxford University Press, New York, 1986.
21 M. Pääkkö, M. Ankerfors, H. Kosonen, A. Nykänen, S. Ahola, M. Osterberg, J. Ruokolainen, J. Laine, P. T. Larsson, O. Ikkala and T. Lindström, *Biomacromolecules*, 2007, **8**, 1934–1941.
22 C. P. Broedersz and F. C. MacKintosh, *Rev. Mod. Phys.*, 2014, **86**, 995–1036.
23 C. P. Broedersz, M. Sheinman and F. C. MacKintosh, *Phys. Rev. Lett.*, 2012, **108**, 078102.
24 M. Sahimi and S. Arbabi, *Phys. Rev. B*, 1993, **47**, 703–712.
25 A. P. Chatterjee, *J. Phys. Condens. Matter*, 2011, **23**, 155104.
26 A. Reuss, *Zeitschrift für Angew. Math. und Mech.*, 1929, **9**, 49–58.
27 W. Voigt, *Ann. Phys.*, 1889, **274**, 573–587.
28 M. A. S. A. Samir, F. Alloin and A. Dufresne, *Biomacromolecules*, 2005, **6**, 612–626.
29 V. Favier, R. Dendievel, G. Canova, J. Y. Cavaille and P. Gilormini, *Acta Mater.*, 1997, **45**, 1557–1565.
30 A. P. Chatterjee, *J. Appl. Phys.*, 2010, **108**.
31 G. M. H. Wilkins, P. T. Spicer and M. J. Solomon, *Langmuir*, 2009, **25**, 8951–8959.
32 M. J. Solomon and P. T. Spicer, *Soft Matter*, 2010, **6**, 1391.